Title: "Real-time county-aggregated wastewater-based estimates for SARS-CoV-2 effective reproduction numbers"

Authors: Sindhu Ravuri[$1], Elisabeth Burnor[1], Isobel Routledge[1], Natalie Linton[1], Mugdha Thakur[1], Alexandria Boehm[2], Marlene Wolfe[3], Heather N. Bischel[4], Colleen C. Naughton[5], Alexander T. Yu[1], Lauren A. White[1] & Tomás M. León[1]

[$]Corresponding author

Affiliations:

[1] California Department of Public Health Center for Infectious Diseases, Richmond and Sacramento, CA, USA
[2] Department of Civil and Environmental Engineering, Stanford University, California, USA
[3] Rollins School of Public Health, Emory University, Atlanta, Georgia, USA
[4] Department of Civil and Environmental Engineering, University of California Davis, Davis, CA, USA
[5] Department of Civil and Environmental Engineering, University of California Merced, Merced, CA, USA

Complete contact information for the corresponding author (name, email address, and postal address):
Sindhu Ravuri; sindhu.ravuri@cdph.ca.gov; 850 Marina Bay Pkwy, Building P, Richmond, CA 94804, USA

Declaration of conflicts of interest:
The authors declare they have no conflicts of interest related to this work to disclose.

ABSTRACT

Background: The effective reproduction number (R_e) serves as a metric of population-wide, time-varying disease spread. During the COVID-19 pandemic, R_e was primarily estimated from clinical surveillance data streams (R_{cc}), which have varied in quality and representativeness due to changes in testing volume, test-seeking behavior, and resource constraints. Deriving R_e from alternative data sources such as wastewater could inform future public health responses.

Objectives: We estimated county-aggregated, sewershed-restricted wastewater-based SARS-CoV-2 R_e (R_{ww}) from May 1, 2022 to April 30, 2023 for five counties in California of varying population sizes, clinical testing rates, demographics, proportions surveilled by wastewater, and sampling frequencies to validate the reliability of R_{ww} as a real-time disease surveillance metric.

Methods: We produced both instantaneous and cohort sewershed-restricted R_e using smoothed and deconvolved wastewater concentrations. We then population-weighted and aggregated these sewershed-level estimates to arrive at county-level R_e. Using mean absolute error (MAE), Spearman's rank correlation (ρ), confusion matrix classification, and cross-correlation analyses, we compared the timing and trajectory of two R_{ww} models to: (1) a publicly available, county-level ensemble of R_{cc} estimates, and (2) a county-aggregated, sewershed-restricted R_{cc}.

Results: Both R_{ww} models demonstrated high concordance with traditional R_{cc} estimates, as indicated by low mean absolute errors (MAE $\leq$ 0.09), significant positive Spearman correlation (Spearman $\rho \geq 0.66$, $p < 0.001$), and high confusion matrix classification accuracy ($\geq$ 0.81). The relative timings of R_{ww} and R_{cc} were less clear, with cross-correlation analyses suggesting strong associations for a wide range of temporal lags that varied by county and R_{ww} model type.

Discussion: This R_e estimation methodology provides a generalizable, robust, and operationalizable framework for estimating county-level R_{ww}. Our results support the additional use of R_{ww} as an epidemiological tool for surveillance. Based on this research, we produced publicly available R_{ww} nowcasts for the California Communicable diseases Assessment Tool (https://calcat.covid19.ca.gov/cacovidmodels/).

INTRODUCTION

The effective reproduction number (R_e) of a disease represents the average number of secondary infections caused by a newly infectious individual within a population of both susceptible and immune hosts.[1] An R_e value greater than one suggests the number of new infections within a population will increase, while an R_e value less than one indicates the number of new infections will decrease.[2] In the context of SARS-CoV-2, R_e commonly serves as a metric of population-wide disease spread under conditions of time-varying vaccination rates, immunity viral variant evolution, health protective behavior modifications, and other response measures.[2] Importantly, monitoring R_e can inform public health policy decisions (e.g., travel restrictions, school closures, mask requirements).[3–6]

In the first years of the COVID-19 pandemic, R_e was estimated from clinical surveillance data streams such as confirmed case counts (i.e., "case-based" R_e). However, the quality and representativeness of clinical data are not always consistent through time and space. Ongoing changes in testing capacity, access, eligibility, test-seeking behavior and reporting may bias case-based R_e estimates; for example, a simulation study mimicking alterations to testing practices found that increasing or decreasing the proportion of detected cases over- or under-estimated R_e, respectively.[7] Delays and administrative noise in case reporting (e.g., lagged processing speed for weekend data) are also common issues for traditional R_e estimation tools.[8] Deriving R_e from alternative data sources will be an important means of informing response to the future public health impact of COVID-19 and bolstering nowcasting efforts.

The COVID-19 pandemic highlighted wastewater surveillance as a timely and accurate monitoring tool reflecting community-wide disease transmission.[9,10] Wastewater surveillance measures the amount of SARS-CoV-2 viral RNA shed into wastewater by infected individuals. It circumvents limitations of traditional clinical SARS-CoV-2 surveillance in important ways. First, it captures both asymptomatic and symptomatic infections.[11] Second, wastewater surveillance is not as impacted by heterogeneous, time- and space-varying testing-related factors.[12–16] Third, wastewater surveillance data is usually available within days, overcoming case reporting delays.[12–16] For these reasons, using wastewater surveillance could improve the accuracy and reliability of R_e estimates while also compensating for data delays from traditional sources. In addition, given that wastewater surveillance measures viral RNA concentrations at the level of a single wastewater treatment plant's catchment area (sewershed), it could be used to estimate real-time R_e in finite geographies that may lack robust case reporting.

Existing methods of wastewater-based R_e (denoted as R_{ww} in this study, following notation by Huisman et al.[17]) estimation include SEIR-like compartmental models,[18] branching process-inspired models,[17,19,20] and artificial neural networks.[21] Despite using different underlying mathematical approaches, these methods have consistently revealed high concordance between R_{ww} and conventional case-based R_e estimates (denoted as R_{cc} in this study, following notation by Huisman et al.[17]). In some circumstances, R_{ww} even highlights outbreak dynamics not captured by R_{cc} alone; for example, Nadeau et al.[20] demonstrated that, compared to R_{cc}, R_{ww} better reflected the impact of COVID-19 interventions on influenza transmission. Notably, these studies have typically examined R_{ww} at the scale of an individual sewershed. However, a single county may contain multiple treatment plants representing distinct communities, and sewersheds do not typically map to municipal boundaries. Moreover, public health policies are often enacted on a county or regional level. Deriving county-level R_{ww} estimates that integrate data from multiple sewersheds would therefore provide a more comprehensive view of community transmission dynamics at a geographic scale relevant for public health policymaking.

In this study, we provide proof-of-concept estimation of county-aggregated, sewershed-restricted R_{ww} for the state of California from May 1, 2022 to April 30, 2023. We compare the timing and trajectory of two R_{ww} models to: (1) a publicly available, county-level ensemble of R_{cc} estimates, and (2) a county-aggregated, sewershed-restricted R_{cc} for SARS-CoV-2 (though it is important to note that R_{ww} and R_{cc} are both measuring an unobservable quantity, R_e, the "true" underlying parameter). To evaluate generalizability of our estimation procedure across distinct populations, we present results for five counties with varying sizes, clinical testing rates, demographics, proportions surveilled by wastewater, and sampling frequencies.

METHODS

R_e Estimation Overall Approach

To produce R_{ww} estimates, we relied on the R_e derivation frameworks developed by Cori et al.[1] and Wallinga & Teunis[22] (hereafter denoted as instantaneous or cohort R_e, respectively). These two modeling approaches, traditionally applied on case data, have been well characterized and broadly used in public health for real-time R_{cc} estimation.[8]

We compared the timing and trajectory of these two R_{ww} models to the following: (1) county-level R_{cc} ensembles sourced from the California Communicable diseases Assessment Tool, CalCAT (https://calcat.covid19.ca.gov/cacovidmodels/) (hereafter denoted as the CalCAT ensemble); and (2) R_{cc} estimates produced by applying Cori et al.[1] and Wallinga & Teunis[22] to sewershed-restricted case data (hereafter denoted as sewershed-restricted R_{cc}). Comparing R_{ww} results to the CalCAT ensemble allows us to validate the robustness and reliability of R_{ww} as a real-time disease surveillance metric for public health. Additionally, comparing R_{ww} results to sewershed-restricted R_{cc} offers two potential advantages. First, sewershed-restricted R_{cc} represents the same populations within a given county as R_{ww}, while the CalCAT ensemble relies on county-wide data sources. Second, sewershed-restricted R_{cc} can be indexed by time of infection. In contrast, the CalCAT ensemble integrates different models with varying R_e estimation procedures, meaning its estimates cannot be easily indexed by time of infection. Therefore, comparing R_{ww} and sewershed-restricted R_{cc} allows us to contextualize the former's timing with respect to conventional case-based approaches.

We first conducted our R_{ww} estimation process using wastewater data. We subsequently repeated the estimation procedure on sewershed-restricted case data to produce R_{cc} (Figure 2). County-level CalCAT ensemble estimates are publicly available and were not further processed. Our analysis period spanned one year (May 1, 2022 to April 30, 2023).

R_e Estimation Process

STEP 0: Raw Data Sources

Wastewater Sampling

Wastewater samples included in the study were collected during the analysis period using two different methods of sample processing, as described below (Table 1). Samples were collected from 14 sewersheds in five California counties at a frequency of three to seven times per week (Table 1). Samples from eight sites (San Francisco Southeast, San Francisco Oceanside, Sacramento, Palo Alto, San Jose, Sunnyvale, Gilroy/Morgan Hill, and Davis) were processed according to Method 1. Samples from six sites (Modesto, Merced, Turlock, Esparto, Winters, and Woodland) were processed according to Method 2 from May 1, 2022 to November 30, 2022 and according to Method 1 from December 1, 2022 until April 30, 2023 (Tables 1 and S1). Method 2 was designed to closely follow the protocol of Method 1, with sample processing and laboratory analyses performed at a different laboratory.

<u>Method 1, Sample Processing</u>

Protocols developed for Method 1 were designed and reported according to the Environmental Microbiology Minimum Information (EMMI) guidelines, as described in Borchardt et al.[23] For samples processed via Method 1, 50 milliliters of wastewater settled solids were collected three to seven times per week from the primary clarifier or from influent using an Imhoff cone,[24,25] transferred at 4°C and processed immediately upon receipt at the lab. The methods used to measure the N gene via digital droplet RT-PCR, including thorough descriptions of the extraction and PCR negative and positive controls, process control recovery, QA/QC elements, thresholding methods, and relevant EMMI guideline reporting, have been described in detail in the Supplemental Materials and in a previously published data descriptor.[26]

Briefly, wastewater settled solids were dewatered with centrifugation and added to DNA/RNA Shield (Zymo Research Corporation, Irvine, CA) at a concentration of 75 mg/ml to minimize inhibition. Nucleic acids were

extracted and quantified by a digital droplet RT-PCR assay (dd-RT-PCR) targeting the N gene of SARS-CoV-2.[26] More detailed methods can be found in the Supplemental Materials.

Method 2, Sample Processing

For samples processed via Method 2, the collection procedure of wastewater solids varied by site (Table 1). For Modesto, grab samples of settled solids from a primary clarifier were collected (similar to Method 1). For Esparto, Turlock, and Woodland, composite samples of influent wastewater were collected, and for Winters, composite samples of raw wastewater were collected from a pump station (Table 1). For sites collecting liquid wastewater samples, solids were obtained by settling the samples in a glass beaker for a minimum of 30 minutes. These settled solids were then processed according to the same protocol described for primary settled solids.[27] For all sites, samples were collected three to five times per week and transferred at 4°C to the laboratory. Settled solids were dewatered, diluted in DNA/RNA Shield (Zymo Research Corporation, Irvine, CA), extracted, and quantified by dd-RT-PCR. Minor differences in the processing of dewatered solids, extraction, and dd-RT-PCR assays between Methods 1 and 2 are described in Kadonsky et al.[27] A comparative interlaboratory analysis of wastewater samples collected from sewersheds in Davis city of Yolo county suggests that data obtained using Methods 1 and 2 are comparable.[27]

In this analysis, we used raw, unadjusted wastewater data in units of copies of SARS-CoV-2 RNA per gram of wastewater solids.

County Selection

For this analysis, we estimated R_{ww} for five California counties: Sacramento, San Francisco, Santa Clara, Stanislaus, and Yolo. We selected counties using similar laboratory methodologies that have one or more site(s) with long wastewater sampling histories (multiple years of available data). Inter-method comparisons of wastewater-derived SARS-CoV-2 concentrations can be highly complex, as quantification is dependent on several unique features of a processing pipeline (e.g., sample type (liquid vs. solids), extraction method and efficiency, assay target selection, quantity of extraction replicates and PCR replicates, laboratory equipment, etc.[28] Although six of our sites underwent laboratory changes and all sites underwent minor changes in methodology during the study period, we sought to avoid some of the complications of inter-method data comparability by including only sites processing settled solids (either grab samples from a primary clarifier or solids settled out from a composite wastewater sample) and only sites using the same assay target for SARS-CoV-2 (see Supplemental Methods).

Wastewater monitoring tends to be more robust in urban locations for reasons such as larger population coverage, proximity to laboratories, and greater plant staffing and resources, resulting in inequitable coverage for rural communities.[29] Therefore, we included counties from both urban (San Francisco, Palo Alto, and Sacramento) and rural areas (Stanislaus and Yolo) (Figures 1 and S1).

We define “coverage” as the proportion of a county’s population that resides within sewersheds that are monitored with wastewater surveillance. Amongst California counties, coverage varies widely, ranging from as low as 10% to as high as 100%. R_{ww} estimates produced for counties with low coverage may be subject to selection bias, as they only account for infections in small subpopulations of the county that are sampled via wastewater monitoring programs. Such R_{ww} estimates may consequently follow a trajectory that does not accurately reflect county-wide infection and transmission dynamics. Due to this concern, we chose counties with at least 50% coverage.

Sewershed-Restricted Case Data

Sewershed shapefiles were generated in collaboration with each of the wastewater treatment plants selected for this analysis. PCR-confirmed COVID-19 case counts reported to the California Department of Public Health (CDPH) were linked with each sewershed using methods described previously.[30] Cases were counted as a function of episode date (earliest of date received, date of diagnosis, date of symptom onset, date of death, or date of specimen collection). The California Health and Human Services (CHHS) Committee for the Protection of Human Subjects (CPHS) determined that use of this data is exempt from review under their criteria.

CalCAT Ensemble

As part of the COVID-19 Response, CDPH developed a R_e nowcast ensemble publicly available on CalCAT (https://calcat.covid19.ca.gov/cacovidmodels/). This nowcast is a smoothed median ensemble of both internally generated and externally contributed models. Median ensembles tend to outperform individual models, as has been demonstrated during the COVID-19 pandemic.[31,32] Smoothing ensures that the ensemble is robust to outliers, dampening noise in the median nowcast. The models are predominantly case-based, though some additionally or instead use test positivity, hospitalizations, intensive care unit census, and/or deaths as an input (Table S2).

The CalCAT ensemble is produced on county, region, and state levels. In this study, we strictly use county-level CalCAT ensemble estimates. The ensemble is retroactively updated for the dates through the present day, based on latest estimates from contributing models. The number and cadence of daily contributor models to the ensemble may vary across time and geographies.

The CalCAT ensemble continues to serve as a real-time disease dynamics monitoring tool informing state policymakers on the speed and strength of SARS-CoV-2 transmission and burden.

STEP 1: Data transformation

Input time series data streams for sewershed-level R_e estimation (i.e., case counts and wastewater viral concentrations) were transformed using distinct approaches to minimize noisiness for each data stream (Figure 2). Case counts were LOESS smoothed using the R package estimateR. Raw wastewater concentrations were spline smoothed using the R package npreg.[33] To fit sewershed-specific smoothing splines, we spaced knots by seven days over the course of the full analysis period. We selected optimal smoothing parameters unique to each sewershed using ordinary cross validation. Smoothed wastewater concentrations were subsequently square root-transformed. Root transformation produced R_{ww} estimates that were more comparable in absolute terms to R_{cc}, as raw wastewater concentrations (which can be as high as 10^6 copies/gram) are often much greater in magnitude and variability than traditional case counts.

STEP 2: Produce sewershed-level R_e

Both instantaneous and cohort R_e models required a time series input of incidence data indexed by date of infection as well as an estimate of the generation time (i.e., the time interval between infections of an infector and their infectee(s)).[1,34] Sewershed-restricted case counts were indexed by episode date, while wastewater concentrations were indexed by date of shedding into wastewater. We re-indexed these data streams to date of infection using deconvolution with input-specific delay distributions. For case data, we derived a delay distribution using the California COVID-19 case registry. As is typical of observational line list data, date of infection was unknown, and date of symptom onset was not available for many cases, in large part due to the presence of mild or asymptomatic infections and reporting practices. Since episode date in the line list was most representative of the date of nucleic acid amplification test (NAAT) result, we approximated episode date as the date of NAAT result. Next, we deconvolved from date of NAAT result to date of infection using two delay distributions: (1) an estimate of the incubation period, based on Aguila-Mejia et al.,[35] and (2) the delay from symptom onset to NAAT result, based on the line list (Table 2). For wastewater, we used the infection to shedding distribution reported by Huisman et al. (Table 2).[17] This distribution was optimized for San Jose, California, and reflects the profile of SARS-CoV-2 RNA viral shedding by an infected individual during the days post-infection. We used the R package estimateR to perform deconvolution through a variant of the Richardson-Lucy expectation-maximization algorithm.[36]

We also used the estimateR package to produce R_e values derived from the Cori et al.[1] method (hereon referred to as instantaneous R_{ww}). estimateR implements a wrapper around the Cori et al.[1] approach and enables repeated R_e estimation on a user-defined number of bootstrap samples built from the input data time series.[36] The distribution of bootstrapped R_e estimates is then used to produce 95% confidence intervals.[36] We generated 1000 bootstrap samples for our study for each location estimate. To produce R_e values derived from the Wallinga and Teunis method (hereon referred to as cohort R_{ww}), we used the R package R0.[37] We applied an adjustment for right-censorship to obtain accurate R_e estimates at the end of the time series.[34,38] With the R0 package, we ran 1000 multinomial simulations at each time step to compute 95% confidence intervals.[37] Both the instantaneous and cohort models exhibit noise in initial R_e estimates (i.e., extreme spikes). To account for this, we trimmed the first week of estimates for each sewershed-level R_e. For both models, we utilized the generation time reported by Manica et al. (Table 2).[39]

STEP 3: Produce county-level R_e via population weighting

Sewershed-restricted R_{ww} and R_{cc} estimates were weighted by population and subsequently aggregated to produce county-level R_e. The aggregation approach is described in Equation [1], where $R_{ww,i}$ represents R_{ww} of sewershed i, Pop_i represents the population size serviced by sewershed i, and n represents the total number of sewersheds enrolled in wastewater monitoring within the relevant county. This aggregation approach ensures sewersheds corresponding to larger or smaller populations have proportional influence on and representation in the county-level R_{ww} estimate.

$$\text{County-level } R_e = \frac{\sum_{i=1}^{n}(R_{ww,i} \times Pop_i)}{\sum_{i=1}^{n}(Pop_i)} \qquad [1]$$

Sewershed population sizes should be considered approximate, as they are estimated by wastewater utilities using unique and non-standardized methodologies.

For Yolo county's R_{cc}, we modified our aggregation approach to accommodate low case counts in sewershed-restricted boundaries. The minimum number of cumulative infections prior to R_e estimation recommended by Cori et al. is 12.[1,36] In certain Yolo sites (Esparto and Winters), the minimum number of cumulative infections prior to R_e estimation on May 1, 2022 (the analysis period start date) was below this threshold. Such low input case counts generated unreliable R_{cc} estimates with extreme sensitivity to small shifts in case incidence. To address this, we combined case counts across all Yolo sites and input this single time series into our R_e estimation procedure.

Only sewersheds with wastewater data available for a given date were included in the county-aggregated R_e estimate for that date. While most sewersheds in our analysis sampled wastewater for the full study period, San Francisco Southeast began sampling on May 20, 2022. As a result, county-aggregated R_{ww} for San Francisco only includes San Francisco Oceanside for the first 19 days of the study period.

We derived confidence intervals for county-level R_{ww} and R_{cc} as population-weighted ensembles of sewershed-level confidence intervals. For each date, we assumed that a sewershed's R_e (R_{ww} or R_{cc}) point estimate served as the mean of a normal (or Gaussian) distribution with 95% confidence intervals matching those estimated for each sewershed. Under this simplifying assumption, we then linearly interpolated the means and variances of sewershed-level normal distributions within a county to produce a combined normal distribution; confidence intervals of this resultant distribution were used for county-level R_{ww} and R_{cc}. This method of linear interpolation of Gaussian distributions has been shown to reduce the error coverage for ensemble estimates.[40,41] Uncertainty estimation for the CalCAT ensemble was not feasible, as contributing models did not all report confidence intervals.

Comparison of R_e trajectories

To evaluate R_{ww} and R_{cc} concordance in magnitude and direction, we calculated the mean absolute error (MAE) and Spearman's rank correlation (ρ). For R_{ww} versus sewershed-restricted R_{cc}, identical R_e models (instantaneous or cohort) were compared.

CalCAT ensemble values provide real-time, ongoing R_{cc} estimates with relevance for statewide public health response, while sewershed-restricted R_{cc} values provide comparative controls for our particular study. Additional analyses characterizing the directional concordance between R_{ww} and the CalCAT ensemble would provide greater evidence of the former's potential real-time public health utility. To that end, we produced multi-class confusion matrices relating R_{ww} to the CalCAT ensemble. Based on magnitude, R_e values were grouped into transmission strength categories for the state of California (<0.7, 0.7-0.9, 0.9-1.1, 1.1-1.3, >1.3, which represent a sharp decrease, decrease, stability, increase, and sharp increase in R_e, respectively). When predicted R_{ww} values and reference CalCAT ensemble values belong to the same category, the confusion matrix marks it an instance of agreement (in this context, CalCAT ensemble values are treated as the source of truth, or actuals). The total frequency of agreement instances for each R_e category are then visualized by the confusion matrix.

We reported the resulting sensitivity, specificity, positive predictive values (PPV), and negative predictive values (NPV) for each R_e category. Sensitivity and specificity reflected the fraction of CalCAT ensemble observations

which were correctly classified by R_{ww} for each R_e category. PPV and NPV reflected the proportion of matching and non-matching classifications for R_{ww} predictions for each R_e category. Here, for a given R_e category, "true positives" indicate reference observations correctly classified by R_{ww} as belonging to the category, and "true negatives" indicate reference observations correctly classified by R_{ww} as not belonging to the category. We also reported the overall accuracy, which summarizes across all R_e categories. The overall accuracy sums the number of R_e predictions correctly classified by R_{ww} and divides that sum by the total number of observations in the time series. These five metrics do not include the categories $R_e < 0.7$ and $R_e > 1.3$ as they had no values during the study period.

We used the R package caret to generate all confusion matrices and corresponding performance metrics.[42]

Comparison of R_e temporalities

We performed cross-correlation between R_{ww} and R_{cc} to identify temporal lags in the former that may be useful predictors of the latter. Cross-correlations were performed for a lag value range of -20 to 20 days (negative lag values: R_{ww} temporally precedes R_{cc}**;** positive lag values: R_{cc} temporally precedes R_{ww}; lag value of zero: R_{ww} is not temporally shifted with respect to R_{cc}).

RESULTS

We produced two SARS-CoV-2 R_{ww} models for five California counties. We then compared the timing, magnitude, and directionality of R_{ww} to the CalCAT ensemble and sewershed-restricted R_{cc}. All results for San Francisco, Santa Clara, and Yolo counties are included in the main text; numerical results for Sacramento and Stanislaus counties are included in the main text and graphical results are in the Supplemental Material.

Comparison of R_e trajectories

R_{ww} tracks closely with R_{cc} over time and geography (Figures 3, S2, and S4). Quantitatively, we found high correspondence between R_{ww} and R_{cc} trajectories for all counties across three analyses: mean absolute error (MAE), Spearman's rank correlation, and confusion matrix classification.

Mean Absolute Error Analysis

When compared against R_{cc} for the entire analysis period, R_{ww} had a low average MAE (MAE $\leq$ 0.09, Table 3). For both instantaneous and cohort R_{ww} models, MAE values relating R_{ww} to CalCAT ensemble estimates were lower (MAE $\leq$ 0.07) than MAE values relating R_{ww} to sewershed-restricted R_{cc} estimates (MAE $\leq$ 0.09). MAE values relating R_{ww} to CalCAT ensemble estimates were lower for instantaneous R_{ww} (MAE $\leq$ .05), while MAE values relating R_{ww} to sewershed-restricted R_{cc} estimates were lower for cohort R_{ww} (MAE $\leq$ 0.06). These results were consistent across all five counties.

Spearman's Rank Correlation Analysis

Over the entire analysis period, R_{ww} estimates were strongly, positively, and significantly correlated with R_{cc} estimates for all five counties (Spearman $\rho \geq 0.62$, $p < 0.001$) (Table 3). For instantaneous R_{ww}, strength of correlation between R_{ww} and CalCAT ensemble estimates was higher (Spearman $\rho \geq 0.78$, $p < 0.001$) than the strength of correlation between R_{ww} and sewershed-restricted R_{cc} estimates (Spearman $\rho \geq 0.66$, $p < 0.001$) in four of five counties. For cohort R_{ww}, strength of correlation between R_{ww} and the CalCAT ensemble (Spearman $\rho \geq 0.62$, $p < 0.001$) did not show a clear pattern in relation to the strength of correlation between R_{ww} and sewershed-restricted R_{cc} estimates (Spearman $\rho \geq 0.66$, $p < 0.001$). Strength of correlation between R_{ww} and the CalCAT ensemble estimates was higher across all counties for the instantaneous R_{ww} model (Spearman $\rho \geq 0.78$, $p < 0.001$). The strength of correlation between R_{ww} and sewershed-restricted R_{cc} estimates was generally higher for the cohort R_{ww} approach (Spearman $\rho \geq 0.62$, $p < 0.001$), with the exceptions of Sacramento and Yolo counties (for which instantaneous R_{ww} demonstrated slightly higher strength of correlation).

Confusion Matrix Analysis

We performed confusion matrix classification analysis, stratified by county and R_{ww} modeling approach, to further characterize the directional concordance between R_{ww} and the CalCAT ensemble (Figures 4 and S3).

The overall classification accuracy of both R_{ww} models was consistently high ($\geq$ 0.79) across all counties; the sole exception to this pattern was Stanislaus, which had a slightly lower overall accuracy for its R_{ww} models ($\geq$ 0.64) (Tables 4 and 5). Overall accuracy for the cohort R_{ww} model was lower as compared to instantaneous R_{ww} for all counties. For all counties and R_{ww} approaches, the total frequency of agreement instances was greatest for the 0.9 to 1.1 R_e (stable) range (Figures 4 and S3).

Across all counties, both R_{ww} models generally demonstrated the greatest sensitivity and PPV for R_e estimates with magnitudes between 0.9 and 1.1 (sensitivity = 0.78-0.99 and 0.70-0.99; PPV = 0.89-0.97 and 0.77-0.95 for instantaneous and cohort, respectively). For all R_e classifications, sensitivity and PPV varied by geography and R_{ww} model type. Interestingly, for R_e estimates between 0.7 and 0.9, the PPV of cohort R_{ww} was incalculable (San Francisco and Yolo) or 0 (Sacramento and Santa Clara) for all counties except Stanislaus (PPV = 0.48). An incalculable PPV indicates there were no R_{ww} predictions within this range; a PPV of 0 indicates R_{ww} never estimated R_e between 0.7 and 0.9 when the CalCAT ensemble did. However, it is important to caveat that there were few (< 20) eligible observations in this category for all counties except Stanislaus.

For R_e estimates between 0.7 and 0.9 or 1.1 and 1.3, all misclassified R_e (i.e., R_e estimates categorized differently by the CalCAT ensemble versus R_{ww}) were estimated to be in the 0.9 to 1.1 range by both R_{ww} models. Consistent with this finding, both R_{ww} models demonstrated the lowest specificity and NPV for the 0.9 to 1.1 category across all

counties (specificity = 0.48-0.86 and 0.17-0.56; NPV = 0.51-0.85 and 0.31-0.67 for instantaneous and cohort, respectively). For R_e estimates between 0.7 and 0.9 or 1.1 and 1.3, the specificity and NPV remained greater than 0.86 and 0.90, respectively, across all counties for both R_{ww} models. We observed inter- and intra- county- and model-dependent variability in relative magnitudes of the four reported metrics (sensitivity, specificity, PPV, NPV) across R_e classifications.

Comparison of R_e temporalities

We calculated cross-correlation with a maximum lag of 20 days between R_{ww} and R_{cc} to numerically evaluate temporal alignment. Across all counties and R_{ww}-R_{cc} pairings, cross-correlation coefficients ranged from 0.65 to 0.93 (CalCAT ensemble: 0.72-0.93 and 0.69-0.89; sewershed-restricted R_{cc}: 0.65-0.87 and 0.67-0.89 for instantaneous and cohort R_{ww}, respectively). We report the range of time lags for cross-correlation coefficients within 0.05 of the maximum observed correlation value (Table 6, Figures S5 and S6). The reported range of time lags were wide and variable across counties, R_{cc} sources (CalCAT ensemble versus sewershed-restricted), and R_{ww} models (instantaneous versus cohort). Importantly, though, nearly all ranges included a lead time of 0 days, when R_{ww} was not temporally shifted with respect to R_{cc} (the two exceptions to this were: (1) instantaneous R_{ww} with respect to sewershed-restricted R_{cc} for Stanislaus county, and (2) cohort R_{ww} with respect to the CalCAT ensemble for Sacramento county); this is consistent with our previous observations of high concordance between non-time-shifted R_{ww} and R_{cc} (Figures 3 and S2, Table 3).

Within each county, the size and bounds (i.e., minimum and maximum) of the reported range of time lags with respect to sewershed-restricted R_{cc} was broadly similar between both R_{ww} models; this was not true for the range of time lags with respect to the CalCAT ensemble, which differs between R_{ww} models (boundaries of ranges with respect to the CalCAT ensemble: -3 to +10 days and -4 to +10 days of lag for instantaneous and cohort, respectively; boundaries of ranges with respect to the CalCAT ensemble: -8 to +3 days and -16 to +1 days of lag for instantaneous and cohort, respectively).

DISCUSSION

We estimated instantaneous and cohort wastewater-based SARS-CoV-2 effective reproduction numbers for five California counties from May 1, 2022 to April 30, 2023. Across counties with varying population characteristics (e.g., demographics, sizes, clinical testing rates) and wastewater surveillance (e.g., sampling frequency, coverage), both instantaneous and cohort R_{ww} models demonstrated high correspondence with traditional R_{cc} models based on sewershed-restricted and county-wide case data. Correspondence was indicated by low average MAE, significant positive Spearman correlation, and high classification accuracy of R_{ww} with respect to R_{cc} for the entire study period (Table 3, Figure 4). These findings align with existing studies on R_{ww} estimation, which consistently reveal high concordance between R_{ww} and R_{cc} estimates across geographies and time.[17,20,21] R_{ww} concordance with the county-level CalCAT ensemble was generally greater than with sewershed-restricted R_{cc} (Table 3).

Our work did not yield clear conclusions on the relative timing of R_{ww} and R_{cc}. Cross correlative analyses suggested strong associations ranging from a lead time of -16 days to a lag time of +10 days, depending on county, R_{cc} source (CalCAT ensemble versus sewershed-restricted), and R_{ww} model type (Table 6). These findings align mixed results in previous studies assessing the temporal alignment between wastewater and clinical surveillance data[43–46]; several factors, such as clinical data completeness, SARS-CoV-2 variant predominance, sewershed location, and population immunity, may influence the strength of wastewater as a leading indicator of disease incidence.

Similar SARS-CoV-2 R_{ww} estimation pipelines are described in Huisman et al.,[17] Amman et al.,[19] and the publicly available "COVID-19 R estimation for California" dashboard by Worden et al. (https://ca-covid-r.info/). Both published studies produce sewershed-level instantaneous R_{ww}, while the dashboard produces county-level cohort R_{ww}. All methods share a general pipeline schema: wastewater time series data is first processed and subsequently fed into an R_e model. However, the methods differ in their strategies for data transformation, deconvolution (including selection of infection to shedding delay distributions), and county aggregation. For data transformation, our method is most similar to Amman et al.,[19] as both implement a spline approach to smooth wastewater data. For deconvolution, our method is most similar to Huisman et al.,[17] as both implement a variant of the Richardson-Lucy expectation-maximization algorithm. For county aggregation, our method differs from that of the "COVID-19 R estimation for California" dashboard (https://ca-covid-r.info/): we perform population weighting of sewershed-level R_{ww}, while the dashboard uses non-population-weighted, county-aggregated input wastewater data to estimate R_{ww}. We chose population-weighting to ensure sewersheds corresponding to larger or smaller populations have proportional influence on and representation in the county-level R_{ww} estimate. We opted for aggregating sewershed-restricted R_{ww} instead of sewershed-restricted raw RNA concentrations because the latter are not necessarily comparable between sewersheds due to environmental conditions and wastewater attributes.

There are several limitations to our study. First and most importantly, to validate R_{ww} we treated R_{cc} as the gold standard R_e metric. However, both clinical and wastewater data streams have their respective strengths and limitations. Clinical data streams are influenced by heterogeneous, time- and space-varying testing-related factors, ultimately capturing only a subset of infections. Wastewater data streams, while independent of some of the biases impacting clinical surveillance, require accurate characterization of the fecal shedding load distribution in order to be interpreted; the temporal dynamics of fecal shedding and its relationship to variant, immunity status, or disease severity, continue to be an ongoing area of investigation.[47–49] Given this uncertainty surrounding fecal shedding, pooled viral concentrations in wastewater are difficult to directly translate into unique infection or transmission events. Consequently, R_{ww} may not truly represent the average number of secondary cases caused by a newly infectious individual. Instead, it may be more indicative of other disease characteristics such as infectiousness (since highest shedding tends to occur when someone is most infectious). This is in contrast to traditional R_{cc} estimates, which use discrete units of disease burden (e.g., case counts) in conjunction with generation time or serial interval distributions to directly reconstruct and quantify transmission events. Ultimately, these limitations suggest that both clinical and wastewater data streams are imperfect proxies for COVID-19 disease dynamics; together though, both sources could potentially offer a more comprehensive picture of transmission dynamics and infection risk. While the present study frames R_{cc} as a gold-standard metric, R_{cc} and R_{ww} should instead be considered as two complementary R_e metrics informed by synergistic data sources.

Second, county-level R_{ww} is based on sewershed-restricted wastewater data. Such data only reflects the shedding patterns and disease conditions of wastewater-surveilled communities and may not be generalizable to the entire county population. This has important implications for the utility of R_{ww} in the context of public health policies, such as health mandates, which are often applied at the county level. Any county-level policies informed by R_{ww} would be

tied to a transmission indicator that can only account for the sewershed-surveilled subset of the infected population. This is especially relevant for the state of California, where most counties (especially those in rural areas) have <50% of the county population surveilled by wastewater. Given that our study focuses on counties with >50% coverage, our findings on the agreement between county-aggregated, sewershed-level R_{ww} and county-level CalCAT ensemble R_{cc} may not translate to communities with lower programmatic wastewater surveillance. In addition, the wastewater-surveilled subset may demonstrate unique behaviors that are not representative of the entire county, potentially biasing R_{ww}.

Third, wastewater data is susceptible to location- or time-specific environmental conditions. Wastewater samples are relatively small volumes of wastewater collected from millions of gallons of organic and inorganic materials flowing through a treatment plant; as such, factors like rainfall, industrial input, temperature, and sewage travel time can impact measured SARS-CoV-2 RNA concentrations. This may weaken R_{ww}–R_{cc} concordance in specific counties.

There are also key limitations within our R_{ww} estimation process. For all five counties in our study, we assume the experimentally inferred, optimized infection to shedding distribution for San Jose described by Huisman et al.[17] This distribution maximized R_{ww}-R_{cc} agreement for a single treatment plant studied by Huisman et al.,[17] and is therefore not reflective of the highly variable fecal shedding profile amongst individuals and populations. This upstream assumption in our pipeline impacts the number of inferred infections per day from wastewater, ultimately influencing R_{ww} estimates. Similarly, specific decisions were made in the estimation process related to smoothing (e.g., methodology), trimming (e.g., width or window), and deconvolution (e.g., choice of incubation period, generation time) which may influence downstream results.

Lastly, it is important to consider practical limitations relevant for operationalization of our methods. Firstly, our study is a retrospective analysis using readily available historical surveillance data that has been updated post hoc as more accurate information was reported. This contrasts with real-time or emergency conditions, when both R_{cc} and R_{ww} can only rely on data available at a given time. As such, real-time operationalization of the R_{ww} estimation procedure outlined in this study may require additional data pre-processing, nowcasting, and forecasting steps in the absence of current data. Secondly, counties were selected for this pilot analysis to prioritize similar laboratorial methodologies, long-term sampling histories, high population coverage by wastewater surveillance, and representation of diverse (rural and urban) demographics. Such historically comprehensive, consistently measured, and frequently sampled wastewater data is not available for all sewersheds, counties, or regions. Therefore, the performance of the R_{ww} estimation process presented here may vary considerably when applied to other jurisdictions in California and may not be generalizable. In the future, investigating R_{ww} estimation in a larger suite of counties and regions will be essential to comprehensively understanding the utility of our method in a wide range of scenarios. Another future extension includes identifying the minimum wastewater county coverage and sampling frequency required for high R_{ww}-R_{cc} concordance, which would increase county representation (building upon initial work done by Huisman et al. 2022 for San Jose). Finally, methodological differences can impact measured wastewater concentrations, which in turn can complicates comparability between sites. While we selected sewersheds using similar laboratory methods for this study, some differences still remained in how wastewater solids were collected, processed, or quantified. We do not have conclusive evidence on the impact of even minor differences in laboratory methodologies on downstream R_{ww} estimation. Moreover, best practices for combining wastewater data across multiple methods and laboratories (either over time for a single site, or for distinct sites within a single county) remain an area of ongoing and future research.

We estimated county-level R_{ww}, which we demonstrated tracks closely with robust traditional case-based R_{cc} estimates. Our results support the future use of R_{ww} as an additional epidemiological tool with public health relevance in the context of disease dynamics monitoring. Moreover, our study provides a generalizable, robust, and operationalizable framework for estimating county-level R_{ww}. On the basis of this research, we produced publicly available SARS-CoV-2 R_{ww} nowcasts for the CalCAT dashboard (https://calcat.covid19.ca.gov/cacovidmodels/), advancing COVID-19 transmission monitoring for the state of California. This study and the described approach can inform other jurisdictions' construction and implementation of sewershed- and county-level R_{ww} estimation pipelines. In the future, the described estimation procedure could be applied to other pathogens with available wastewater and case surveillance data (e.g., respiratory syncytial virus [RSV], influenza).

REFERENCES

1. New Framework and Software to Estimate Time-Varying Reproduction Numbers During Epidemics | American Journal of Epidemiology | Oxford Academic. Accessed November 21, 2023. https://academic.oup.com/aje/article/178/9/1505/89262?login=false

2. Joint Research Centre (European Commission), Annunziato A, Asikainen T. *Effective Reproduction Number Estimation from Data Series*. Publications Office of the European Union; 2020. Accessed November 21, 2023. https://data.europa.eu/doi/10.2760/036156

3. Linka K, Peirlinck M, Kuhl E. The reproduction number of COVID-19 and its correlation with public health interventions. *Comput Mech*. 2020;66(4):1035-1050. doi:10.1007/s00466-020-01880-8

4. Fauci AS, Lane HC, Redfield RR. Covid-19 — Navigating the Uncharted. *N Engl J Med*. 2020;382(13):1268-1269. doi:10.1056/NEJMe2002387

5. Dainton C, Hay A. Quantifying the relationship between lockdowns, mobility, and effective reproduction number (Rt) during the COVID-19 pandemic in the Greater Toronto Area. *BMC Public Health*. 2021;21(1):1658. doi:10.1186/s12889-021-11684-x

6. Inglesby TV. Public Health Measures and the Reproduction Number of SARS-CoV-2. *JAMA*. 2020;323(21):2186-2187. doi:10.1001/jama.2020.7878

7. Pitzer VE, Chitwood M, Havumaki J, et al. The Impact of Changes in Diagnostic Testing Practices on Estimates of COVID-19 Transmission in the United States. *Am J Epidemiol*. Published online April 8, 2021:kwab089. doi:10.1093/aje/kwab089

8. Nash RK, Nouvellet P, Cori A. Real-time estimation of the epidemic reproduction number: Scoping review of the applications and challenges. *PLOS Digit Health*. 2022;1(6):e0000052. doi:10.1371/journal.pdig.0000052

9. Li X, Zhang S, Sherchan S, et al. Correlation between SARS-CoV-2 RNA concentration in wastewater and COVID-19 cases in community: A systematic review and meta-analysis. *J Hazard Mater*. 2023;441:129848. doi:10.1016/j.jhazmat.2022.129848

10. Rabe A, Ravuri S, Burnor E, et al. Correlation between wastewater and COVID-19 case incidence rates in major California sewersheds across three variant periods. *J Water Health*. 2023;21(9):1303-1317. doi:10.2166/wh.2023.173

11. Bivins A, North D, Ahmad A, et al. Wastewater-Based Epidemiology: Global Collaborative to Maximize Contributions in the Fight Against COVID-19. *Environ Sci Technol*. 2020;54(13):7754-7757. doi:10.1021/acs.est.0c02388

12. Peccia J, Zulli A, Brackney DE, et al. Measurement of SARS-CoV-2 RNA in wastewater tracks community infection dynamics. *Nat Biotechnol*. 2020;38(10):1164-1167. doi:10.1038/s41587-020-0684-z

13. Wolfe MK, Topol A, Knudson A, et al. High-Frequency, High-Throughput Quantification of SARS-CoV-2 RNA in Wastewater Settled Solids at Eight Publicly Owned Treatment Works in Northern California Shows Strong Association with COVID-19 Incidence. *mSystems*. 2021;6(5):10.1128/msystems.00829-21. doi:10.1128/msystems.00829-21

14. Kirby AE, Walters MS, Jennings WC, et al. Using Wastewater Surveillance Data to Support the COVID-19 Response — United States, 2020–2021. *Morb Mortal Wkly Rep*. 2021;70(36):1242-1244. doi:10.15585/mmwr.mm7036a2

15. Olesen SW, Imakaev M, Duvallet C. Making waves: Defining the lead time of wastewater-based epidemiology for COVID-19. *Water Res*. 2021;202:117433. doi:10.1016/j.watres.2021.117433

16. Zhu Y, Oishi W, Maruo C, et al. Early warning of COVID-19 via wastewater-based epidemiology: potential and bottlenecks. *Sci Total Environ*. 2021;767:145124. doi:10.1016/j.scitotenv.2021.145124

17. Huisman JS, Scire J, Caduff L, et al. Wastewater-Based Estimation of the Effective Reproductive Number of SARS-CoV-2. *Environ Health Perspect*. 2022;130(5):057011. doi:10.1289/EHP10050

18. Nourbakhsh S, Fazil A, Li M, et al. A wastewater-based epidemic model for SARS-CoV-2 with application to three Canadian cities. *Epidemics*. 2022;39:100560. doi:10.1016/j.epidem.2022.100560

19. Amman F, Markt R, Endler L, et al. Viral variant-resolved wastewater surveillance of SARS-CoV-2 at national scale. *Nat Biotechnol*. 2022;40(12):1814-1822. doi:10.1038/s41587-022-01387-y

20. Nadeau S, Devaux AJ, Bagutti C, et al. Influenza transmission dynamics quantified from wastewater. Published online January 25, 2023:2023.01.23.23284894. doi:10.1101/2023.01.23.23284894

21. Jiang G, Wu J, Weidhaas J, et al. Artificial neural network-based estimation of COVID-19 case numbers and effective reproduction rate using wastewater-based epidemiology. *Water Res*. 2022;218:118451. doi:10.1016/j.watres.2022.118451

22. Wallinga J, Teunis P. Different epidemic curves for severe acute respiratory syndrome reveal similar impacts of control measures. *Am J Epidemiol*. 2004;160(6):509-516. doi:10.1093/aje/kwh255

23. Borchardt MA, Boehm AB, Salit M, Spencer SK, Wigginton KR, Noble RT. The Environmental Microbiology Minimum Information (EMMI) Guidelines: qPCR and dPCR Quality and Reporting for Environmental Microbiology. *Environ Sci Technol*. 2021;55(15):10210-10223. doi:10.1021/acs.est.1c01767

24. Kim S, C. Kennedy L, K. Wolfe M, et al. SARS-CoV-2 RNA is enriched by orders of magnitude in primary settled solids relative to liquid wastewater at publicly owned treatment works. *Environ Sci Water Res Technol*. 2022;8(4):757-770. doi:10.1039/D1EW00826A

25. Wolfe MK, Archana A, Catoe D, et al. Scaling of SARS-CoV-2 RNA in Settled Solids from Multiple Wastewater Treatment Plants to Compare Incidence Rates of Laboratory-Confirmed COVID-19 in Their Sewersheds. *Environ Sci Technol Lett*. 2021;8(5):398-404. doi:10.1021/acs.estlett.1c00184

26. Boehm AB, Wolfe MK, Wigginton KR, et al. Human viral nucleic acids concentrations in wastewater solids from Central and Coastal California USA. *Sci Data*. 2023;10(1):396. doi:10.1038/s41597-023-02297-7

27. Kadonsky KF, Naughton CC, Susa M, et al. Expansion of wastewater-based disease surveillance to improve health equity in California's Central Valley: sequential shifts in case-to-wastewater and hospitalization-to-wastewater ratios. *Front Public Health*. 2023;11. Accessed November 21, 2023. https://www.frontiersin.org/articles/10.3389/fpubh.2023.1141097

28. M. Pecson B, Darby E, N. Haas C, et al. Reproducibility and sensitivity of 36 methods to quantify the SARS-CoV-2 genetic signal in raw wastewater: findings from an interlaboratory methods evaluation in the U.S. *Environ Sci Water Res Technol*. 2021;7(3):504-520. doi:10.1039/D0EW00946F

29. Medina CY, Kadonsky KF, Roman FA, et al. The need of an environmental justice approach for wastewater based epidemiology for rural and disadvantaged communities: A review in California. *Curr Opin Environ Sci Health*. 2022;27:100348. doi:10.1016/j.coesh.2022.100348

30. Yu AT, Hughes B, Wolfe MK, et al. Estimating Relative Abundance of 2 SARS-CoV-2 Variants through Wastewater Surveillance at 2 Large Metropolitan Sites, United States. *Emerg Infect Dis*. 2022;28(5):940-947. doi:10.3201/eid2805.212488

31. White LA, McCorvie R, Crow D, Jain S, León TM. Assessing the accuracy of California county level COVID-19 hospitalization forecasts to inform public policy decision making. *BMC Public Health*. 2023;23(1):782. doi:10.1186/s12889-023-15649-0

32. Evaluation of individual and ensemble probabilistic forecasts of COVID-19 mortality in the United States | PNAS. Accessed November 21, 2023. https://www.pnas.org/doi/abs/10.1073/pnas.2113561119

33. Helwig N. npreg: Nonparametric Regression via Smoothing Splines. Published online 2022. https://CRAN.R-project.org/package=npreg

34. Gostic KM, McGough L, Baskerville EB, et al. Practical considerations for measuring the effective reproductive number, Rt. *PLOS Comput Biol*. 2020;16(12):e1008409. doi:10.1371/journal.pcbi.1008409

35. Del Águila-Mejía J, Wallmann R, Calvo-Montes J, Rodríguez-Lozano J, Valle-Madrazo T, Aginagalde-Llorente A. Secondary Attack Rate, Transmission and Incubation Periods, and Serial Interval of SARS-CoV-2 Omicron Variant, Spain. *Emerg Infect Dis*. 2022;28(6):1224-1228. doi:10.3201/eid2806.220158

36. Scire J, Huisman JS, Grosu A, et al. estimateR: an R package to estimate and monitor the effective reproductive number. *BMC Bioinformatics*. 2023;24(1):310. doi:10.1186/s12859-023-05428-4

37. Pierre-Yves Boelle, Obadia T. R0: Estimation of R0 and Real-Time Reproduction Number from Epidemics. Published online 2023. https://CRAN.R-project.org/package=R0

38. Cauchemez S, Boëlle PY, Thomas G, Valleron AJ. Estimating in Real Time the Efficacy of Measures to Control Emerging Communicable Diseases. *Am J Epidemiol*. 2006;164(6):591-597. doi:10.1093/aje/kwj274

39. Manica M, Bellis AD, Guzzetta G, et al. Intrinsic generation time of the SARS-CoV-2 Omicron variant: An observational study of household transmission. *Lancet Reg Health – Eur*. 2022;19. doi:10.1016/j.lanepe.2022.100446

40. Ahmadi J, Basiri E, Kundu D. Confidence and prediction intervals based on interpolated records. *J Nonparametric Stat*. 2017;29(1):1-21. doi:10.1080/10485252.2016.1239826

41. Beutner E, Cramer E. Using linear interpolation to reduce the order of the coverage error of nonparametric prediction intervals based on right-censored data. *J Multivar Anal*. 2014;129:95-109. doi:10.1016/j.jmva.2014.04.007

42. Kuhn M. caret: Classification and Regression Training. Published online 2022. https://CRAN.R-project.org/package=caret

43. Hegazy N, Cowan A, D'Aoust PM, et al. Understanding the dynamic relation between wastewater SARS-CoV-2 signal and clinical metrics throughout the pandemic. *Sci Total Environ*. 2022;853:158458. doi:10.1016/j.scitotenv.2022.158458

44. Duvallet C, Wu F, McElroy KA, et al. Nationwide Trends in COVID-19 Cases and SARS-CoV-2 RNA Wastewater Concentrations in the United States. *ACS EST Water*. 2022;2(11):1899-1909. doi:10.1021/acsestwater.1c00434

45. Li L, Mazurowski L, Dewan A, et al. Longitudinal monitoring of SARS-CoV-2 in wastewater using viral genetic markers and the estimation of unconfirmed COVID-19 cases. *Sci Total Environ*. 2022;817:152958. doi:10.1016/j.scitotenv.2022.152958

46. Morvan M, Jacomo AL, Souque C, et al. An analysis of 45 large-scale wastewater sites in England to estimate SARS-CoV-2 community prevalence. *Nat Commun*. 2022;13(1):4313. doi:10.1038/s41467-022-31753-y

641 47. Hoffmann T, Alsing J. *Faecal Shedding Models for SARS-CoV-2 RNA amongst Hospitalised Patients and*
642 *Implications for Wastewater-Based Epidemiology*. Infectious Diseases (except HIV/AIDS); 2021.
643 doi:10.1101/2021.03.16.21253603

644 48. Crank K, Chen W, Bivins A, Lowry S, Bibby K. Contribution of SARS-CoV-2 RNA shedding routes to RNA
645 loads in wastewater. *Sci Total Environ*. 2022;806:150376. doi:10.1016/j.scitotenv.2021.150376

646 49. Arts PJ, Kelly JD, Midgley CM, et al. Longitudinal and quantitative fecal shedding dynamics of SARS-CoV-2,
647 pepper mild mottle virus, and crAssphage. *mSphere*. 2023;8(4):e00132-23. doi:10.1128/msphere.00132-23

648 50. Topol A. *High Throughput Pre-Analytical Processing of Wastewater Settled Solids for SARS-CoV-2 RNA*
649 *Analyses V2*.; 2021. doi:10.17504/protocols.io.b2kmqcu6

650 51. Sciences) AT (Verily L, Sciences) BW (Verily L, Michigan) KW (Univ, Boehm AB, marlene.wolfe. High
651 Throughput SARS-COV-2, PMMOV, and BCoV quantification in settled solids using digital RT-PCR.
652 Published online April 21, 2021. Accessed November 22, 2023. https://www.protocols.io/view/high-
653 throughput-sars-cov-2-pmmov-and-bcov-quantifi-btywnpxe

654 52. Boehm AB, Wolfe MK, White B, Hughes B, Duong D. Divergence of wastewater SARS-CoV-2 and reported
655 laboratory-confirmed COVID-19 incident case data coincident with wide-spread availability of at-home
656 COVID-19 antigen tests. *PeerJ*. 2023;11:e15631. doi:10.7717/peerj.15631

657

ACKNOWLEDGEMENTS

The wastewater sampling conducted through Method 1 was supported by gifts from the CDC Foundation and the Sergey Brin Family Foundation to ABB. Additional research support for Method 2 were provided through a philanthropic gift to the University of California, Davis. CDPH wastewater surveillance efforts are supported in part by the Epidemiology and Laboratory Capacity for Infectious Diseases Cooperative Agreement (no. 6NU50CK000539-04-02) from CDC.

The authors sincerely thank the operators at Sacramento Regional Wastewater Treatment Plan, Esparto Wastewater Treatment Facility, Woodland Water Pollution Control Facility, Winters Water Treatment Facility, City of Davis Wastewater Treatment Plant, Modesto's Sutter Primary Treatment Facility, Turlock Regional Water Quality Control Facility, Silicon Valley Clean Water, San Jose Santa Clara Regional Wastewater Facility, City of Sunnyvale Water Pollution Control Plant, Palo Alto Regional Water Quality Control Plant, South County Regional Wastewater Authority, Oceanside Water Pollution Control Plant, and Southeast Water Pollution Control Plant for providing wastewater samples.

The authors further thank the modeling and wastewater surveillance sections at CDPH for input and guidance on the data sources and procedure for R_{ww} estimation outlined in this study.

DATA SHARING

All wastewater data used in this study is publicly accessible through the CA Open Data Portal at https://data.ca.gov/dataset/covid-19-wastewater-surveillance-data-california. Models contributing to the CalCAT ensemble also use data publicly accessible through the CA Open Data Portal, such as downloadable case counts, hospitalizations, deaths and test positivity (https://data.chhs.ca.gov/organization/california-department-of-public-health). Sewershed-restricted COVID-19 case data reported to CDPH is not publicly available; readers should contact the corresponding author with data requests.

PUBLICATION POLICY DISCLAIMER

The findings and conclusions in this article are those of the author(s) and do not necessarily represent the views or opinions of the California Department of Public Health or the California Health and Human Services Agency.

688 **TABLES**

689

690 **Table 1. Population and sampling characteristics of counties and wastewater treatment plants included in the**
691 **analyses.**

County	Wastewater Treatment Plant	Monitoring Lab	Population Served by WW Treatment Plant	County Population Size	Coverage	Median Weekly County Testing Rate (per 100,000)	WW Sample Type	Median WW Weekly Sampling Frequency	Total WW Samples
Sacramento	Sacramento	Method 1	1,480,000	1,570,000	0.94	1,160	Primary settled solids	7	366
San Francisco	San Francisco Southeast	Method 1	750,000	890,000	1	2,040	Primary settled solids	7	340
	San Francisco Oceanside	Method 1	250,000	890,000	1	2,040	Primary settled solids	7	354
Santa Clara	Palo Alto	Method 1	236,000	1,970,000	1	2,175	Primary settled solids	7	366
	Gilroy/Morgan Hill	Method 1	110,338	1,970,000	1	2,175	Primary settled solids	7	366
	San Jose	Method 1	1,500,000	1,970,000	1	2,175	Primary settled solids	7	366
	Sunnyvale	Method 1	153,000	1,970,000	1	2,175	Primary settled solids	7	362
Stanislaus	Modesto	Method 2: May 1 – Nov 30, 2022 Method 1: Dec 1, 2022 – May 1, 2023	230,000	550,000	0.57	1,090	Primary settled solids	Method 2: 4 Method 1: 3	198
	Turlock	Method 2: May 1 – Nov 30, 2022 Method 1: Dec 1, 2022 – May 1, 2023	86,000	550,000	0.57	1,090	Solids settled from 24-hour time-weighted composite influent	Method 2: 4 Method 1: 3	198

Yolo	Davis	Method 1	70,717	220,000	0.63	2,230	Primary settled solids	7	298
	Esparto	Method 2: May 1 – Nov 30, 2022 Method 1: Dec 1, 2022 – May 1, 2023	3,272	220,000	0.63	2,230	Solids settled from 24-hour time-weighted composite influent	Method 2: 4 Method 1: 3	186
	Winters	Method 2: May 1 – Nov 30, 2022 Method 1: Dec 1, 2022 – May 1, 2023	7,285	220,000	0.63	2,230	Solids settled from raw, composite wastewater from pump station	Method 2: 4 Method 1: 3	184
	Woodland	Method 2: May 1 – Nov 30, 2022 Method 1: Dec 1, 2022 – May 1, 2023	59,000	220,000	0.63	2,230	Solids settled from 24-hour time-weighted composite influent	Method 2: 4 Method 1: 3	196

Note: Counties and wastewater treatment plants included in this study were selected based on consistency in laboratory methodology (Methods 1 and 2 both process wastewater settled solids and utilized laboratory protocols designed to be similar), high (>50%) coverage (proportion of the county's population that reside within sewersheds contributing to wastewater monitoring data), and representation of diverse demographics (urban and rural). Samples from six sites (Modesto, Merced, Turlock, Esparto, Winters, and Woodland) were processed via Method 2 for the first part of the study period, followed by Method 1 for the remaining part of the study period. Abbreviations: WW, wastewater

Table 2. Key distribution parameters used in sewershed-level R_e estimation pipeline.

Distribution	Purpose	Relevant R_e	Distribution Type	Mean (SD)	Distribution Parameters	Source
Generation time	Sewershed-restricted R_e estimation from input time series	R_{ww}; sewershed-restricted R_{cc}	Gamma	6.84 (4.48)	Shape: 2.33 Scale: 2.93	Manica et al.[39]
Infection to shedding	Deconvolution of wastewater concentrations	R_{ww}	Gamma	5 (0.5)	Shape: 100 Scale: 0.05	Huisman et al.[17]
Incubation period	Deconvolution of sewershed-restricted case counts	sewershed-restricted R_{cc}	Lognormal	3.1 (2.6)	Meanlog: 0.87 Sdlog: 0.73	Aguila-Mejia et al.[35]
Onset to NAAT result	Deconvolution of sewershed-restricted case counts	sewershed-restricted R_{cc}	Lognormal	3.35 (2.84)	Meanlog: 0.94 Sdlog: 0.73	CA cases line list

Note: Estimation of instantaneous and cohort sewershed-level R_e requires a user-specified generation time distribution. Estimation also requires a time series input of incidence data indexed by date of infection. To index both raw sewershed-restricted case counts and wastewater viral concentrations by date of infection, we performed deconvolution. For cases, we deconvolved using two delay distributions. For wastewater, we deconvolved using a single delay distribution optimized for San Jose, California. Abbreviations: NAAT, nucleic acid amplification test, R_e, effective reproduction number; R_{ww}, sewershed-restricted, wastewater-based effective reproduction number; R_{cc}, case-based effective reproduction number; SD, standard deviation.

Table 3. Comparative analyses of county-level R_{ww} and R_{cc} trajectories using mean absolute error and Spearman's rank correlation.

County	Type of R_{cc} estimate	MAE, Instantaneous R_{ww}	MAE, Cohort R_{ww}	Spearman's ρ, Instantaneous R_{ww}	ρ p-value, Instantaneous R_{ww}	Spearman's ρ, Cohort R_{ww}	ρ p-value, Cohort R_{ww}
Sacramento	Sewershed-restricted cases	0.082	0.072	0.719	3.20E-59	0.712	8.80E-58
	CalCAT ensemble	0.042	0.052	0.775	3.10E-74	0.621	2.30E-40
San Francisco	Sewershed-restricted cases	0.077	0.071	0.726	5.30E-61	0.754	3.10E-68
	CalCAT ensemble	0.025	0.031	0.936	3.80E-167	0.866	2.50E-111
Santa Clara	Sewershed-restricted cases	0.064	0.059	0.800	1.20E-82	0.823	5.50E-91
	CalCAT ensemble	0.028	0.043	0.843	9.10E-100	0.668	1.70E-48
Stanislaus	Sewershed-restricted cases	0.087	0.066	0.779	1.30E-75	0.873	1.60E-115
	CalCAT ensemble	0.052	0.065	0.775	2.20E-74	0.662	2.50E-47
Yolo	Sewershed-restricted cases	0.081	0.073	0.657	2.10E-46	0.658	1.30E-46
	CalCAT ensemble	0.016	0.019	0.891	3.20E-126	0.884	1.10E-121

Note: By calculating mean absolute errors and Spearman's rank correlations, we compared the magnitude and direction of instantaneous and cohort R_{ww} models to two types of R_{cc} estimates: (1) a publicly available ensemble of county-wide R_{cc} estimates ("CalCAT ensemble"), and (2) a county-aggregated, sewershed-restricted R_{cc}. Reported p-values correspond to Spearman's rank correlation, ρ (R_{ww} compared against R_{cc}). Abbreviations: R_{ww}, sewershed-restricted, wastewater-based effective reproduction number; R_{cc}, case-based effective reproduction number; MAE, mean absolute error; ρ (rho), Spearman's rank correlation coefficient.

Table 4. Summary metrics from multi-class confusion matrix analysis evaluating agreement between instantaneous R_{ww} and the CalCAT ensemble.

County	R_e Classification	Overall Accuracy	Sensitivity	Specificity	PPV	NPV
Sacramento	0.7-0.9	0.87	0.73	0.89	0.17	0.99
	0.9-1.1	[a]	0.87	0.84	0.97	0.51
	1.1-1.3		0.87	0.99	0.94	0.98
San Francisco	0.7-0.9	0.89	0.32	0.99	0.75	0.96
	0.9-1.1		0.93	0.64	0.95	0.57
	1.1-1.3		0.86	0.94	0.53	0.99
Santa Clara	0.7-0.9	0.90	0.75	0.95	0.32	0.99
	0.9-1.1		0.90	0.86	0.97	0.63
	1.1-1.3		0.89	0.97	0.79	0.98
Stanislaus	0.7-0.9	0.76	0.95	0.94	0.73	0.99
	0.9-1.1		0.78	0.79	0.89	0.63
	1.1-1.3		0.52	0.88	0.46	0.9
Yolo	0.7-0.9	0.96	0	1	[b]*NA*	0.98
	0.9-1.1		0.99	0.48	0.97	0.85
	1.1-1.3		0.65	0.99	0.85	0.98

Note: We produced multi-class confusion matrices relating instantaneous R_{ww} to the CalCAT ensemble (real-time, ongoing R_{cc} estimates with relevance for statewide public health). R_e values were classified into transmission strength categories based on magnitude (<0.7-0.9, 0.9-1.1, 1.1-1.3, >1.3, which represent a strong decrease, decrease, stability, increase, and strong increase in transmission, respectively). The resulting sensitivity, specificity, positive predictive and negative predictive values for each R_e category are reported. The overall accuracy for each county-level R_{ww} is also reported. We did not report two R_e categories (< 0.7, >1.3), which had no observations during the study period. [a]All gray boxes indicate values identical to the closest, previous non-zero entry within the same column. [b]*NA* entries correspond to R_e categories with zero R_{ww} predictions during the study period. R_e, effective reproduction number; PPV, Positive Predictive Value; NPV, Negative Predictive Value.

Table 5. Summary metrics from multi-class confusion matrix analysis evaluating agreement between cohort R_{ww} and the CalCAT ensemble.

County	R_e Classification	Overall Accuracy	Sensitivity	Specificity	PPV	NPV
Sacramento	0.7-0.9	0.79	0	0.87	0	0.97
	0.9-1.1	[a]	0.84	0.46	0.91	0.31
	1.1-1.3		0.59	0.98	0.82	0.95
San Francisco	0.7-0.9	0.85	0	1	[b]*NA*	0.95
	0.9-1.1		0.93	0.28	0.9	0.38
	1.1-1.3		0.46	0.94	0.38	0.95
Santa Clara	0.7-0.9	0.82	0	0.95	0	0.97
	0.9-1.1		0.89	0.46	0.89	0.44
	1.1-1.3		0.57	0.95	0.63	0.94
Stanislaus	0.7-0.9	0.64	0.54	0.89	0.48	0.91
	0.9-1.1		0.70	0.56	0.77	0.47
	1.1-1.3		0.5	0.86	0.41	0.9
Yolo	0.7-0.9	0.94	0	1	*NA*	0.98
	0.9-1.1		0.99	0.17	0.95	0.67
	1.1-1.3		0.24	0.99	0.67	0.96

Note: We produced multi-class confusion matrices relating instantaneous R_{ww} to the CalCAT ensemble (real-time, ongoing R_{cc} estimates with relevance for statewide public health). R_e values were classified into transmission strength categories based on magnitude (<0.7-0.9, 0.9-1.1, 1.1-1.3, >1.3, which represent a strong decrease, decrease, stability, increase, and strong increase in R_e, respectively). The resulting sensitivity, specificity, positive predictive and negative predictive values for each R_e category are reported. The overall accuracy for each county-level R_{ww} is also reported. We did not report two R_e categories (< 0.7, >1.3), which had no observations during the study period. [a]All gray boxes indicate values identical to the closest, previous non-zero entry within the same column. [b]*NA* entries correspond to R_e categories with zero R_{ww} values during the study period. R_e, effective reproduction number; PPV, Positive Predictive Value; NPV, Negative Predictive Value.

Table 6. Comparison of R_e temporality via cross correlations.

County	R_{cc}	Lag (Days), Instantaneous R_{ww}	Lag (Days), Cohort R_{ww}	CC, Instantaneous R_{ww}	CC, Cohort R_{ww}
Sacramento	Sewershed-restricted cases	[-3, 4]	[-4, 3]	[0.65, 0.7]	[0.67, 0.72]
	CalCAT ensemble	[-8, 2]	[-15, -4]	[0.72, 0.77]	[0.69, 0.73]
San Francisco	Sewershed-restricted cases	[0, 8]	[0, 10]	[0.73, 0.77]	[0.76, 0.80]
	CalCAT ensemble	[-4, 2]	[-11, 0]	[0.87, 0.92]	[0.84, 0.89]
Santa Clara	Sewershed-restricted cases	[-2, 3]	[-3, 4]	[0.84, 0.87]	[0.84, 0.89]
	CalCAT ensemble	[-8, 1]	[-16, -6]	[0.84, 0.88]	[0.8, 0.84]
Stanislaus	Sewershed-restricted cases	[4, 10]	[-1, 7]	[0.72, 0.76]	[0.81, 0.85]
	CalCAT ensemble	[-6, 2]	[-15, -6]	[0.73, 0.76]	[0.78, 0.83]
Yolo	Sewershed-restricted cases	[-2, 9]	[-2, 10]	[0.68, 0.73]	[0.68, 0.73]
	CalCAT ensemble	[-5, 3]	[-9, 1]	[0.88, 0.93]	[0.84, 0.89]

Note: Using cross-correlation analysis with a maximum lag of 20 days, we investigated temporal alignment of R_{ww} (cohort or instantaneous) and R_{cc}. R_{cc} included either the CalCAT ensemble – a publicly available ensemble of county-wide R_{cc} estimates – or county-aggregated, sewershed-restricted R_{cc} estimates. We report the range of time lags for cross-correlation coefficients within 0.05 of the maximum observed correlation value. We also include the range of cross-correlation coefficients within 0.05 of the maximum observed correlation value. Negative lag values indicate R_{ww} temporally precedes R_{cc}**;** positive lag values indicate R_{cc} temporally precedes R_{ww}**;** lag values of zero indicate no temporal shift of R_{ww} with respect to R_{cc}. R_{ww}, sewershed-restricted, wastewater-based effective reproduction number; R_{cc}, case-based effective reproduction number; CC, cross-correlation coefficient

FIGURE CAPTIONS

Figure 1. Map of sewersheds included in analysis.
The geographical boundaries of sewersheds (a wastewater treatment plant's catchment area) selected for the present study are highlighted in blue. Each sewershed's respective county is outlined in black. Three of the five studied counties (San Francisco, Santa Clara, and Yolo) are illustrated; maps of the remaining counties (Sacramento and Stanislaus) are included in the Supplemental Material.

Figure 2. Stepwise process of county-aggregated, sewershed-restricted R_e estimation for a single location.
Using San Francisco as an example, we demonstrate our stepwise pipeline for estimating county-aggregated, sewershed-restricted R_e. Each column represents a single wastewater treatment plant within the county. The left column corresponds to San Francisco Oceanside, which surveils 28% of the total county population; the right column corresponds to San Francisco Southeast, which surveils 84% of the total county population. Detailed axes are excluded for this generic, representation of the R_e estimation process. (A) The pipeline begins with raw, sewershed-restricted time series data; in our study, input data includes case counts (pink) and wastewater viral concentrations (blue). (B) In Step 1, raw time series data are transformed: case counts are LOESS smoothed, while wastewater concentrations are spline smoothed and root transformed. Transformed data are subsequently deconvolved, shifting both time series' backwards temporally such that observations are indexed by date of infection. (C) In Step 2, the methods of Cori et al.[1] and Wallinga and Teunis[22] are applied on the modified time series data streams to produce instantaneous and cohort sewershed-level R_e estimates. (D) Finally, in Step 4, sewershed-level R_e estimates are population-weighted and aggregated to yield county-level R_e estimates. Note: WW, wastewater surveillance data; R_e, effective reproduction number; Model, R_e modeling approach (instantaneous or cohort).

Figure 3. Time series of county-aggregated, sewershed-restricted R_e for Santa Clara, San Francisco, and Yolo.
Between May 1, 2022 and April 30, 2023, three county-level R_e time series are compared: (top, black) the CalCAT ensemble – a publicly available ensemble of county-wide R_{cc} estimates; (middle, pink) county-aggregated, sewershed-restricted R_{cc}; and (bottom, blue) R_{ww}. Both R_{ww} and sewershed-restricted R_{cc} were calculated using the R_e estimation pipeline piloted in this study. Solid pink or blue lines indicate instantaneous R_e, while dashed pink or blue lines indicate cohort R_e. 95% confidence intervals for each R_e type (instantaneous or cohort) are depicted. Results for three of five studied counties (San Francisco, Santa Clara, and Yolo) are included; results for the remaining counties (Sacramento and Stanislaus) are included in the Supplemental Material. Note: R_{ww}, sewershed-restricted, wastewater-based effective reproduction number; R_{cc}, case-based effective reproduction number.

Figure 4. Frequency of agreement between R_{ww} and the CalCAT ensemble for Santa Clara, San Francisco and Yolo.
Based on magnitude, R_e values were classified into transmission strength categories (<0.7-0.9, 0.9-1.1, 1.1-1.3, >1.3, which represent a strong decrease, decrease, stability, increase, and strong increase in R_e, respectively). Frequency of agreement between R_{ww} and the CalCAT ensemble (i.e., instances when predicted R_{ww} values and reference CalCAT ensemble values belong to the same R_e category) are visualized by the confusion matrix. The right column illustrates results for cohort R_{ww}, and the left for instantaneous R_{ww}. Each row represents a single county. The counter diagonals (top right to bottom left) of each matrix represents true positives. Off-diagonal values indicate instances of disagreement between R_{ww} model predictions and the CalCAT ensemble. Two R_e categories (R_e < 0.7, R_e >1.3) with no R_e values during the study period were excluded. Results for three of five studied counties (San Francisco, Santa Clara, and Yolo) are included; results for the remaining counties (Sacramento and Stanislaus) are included in the Supplemental Material. Note: R_{ww}, sewershed-restricted, wastewater-based effective reproduction number; Instantaneous, instantaneous R_{ww}; Cohort, cohort R_{ww}.

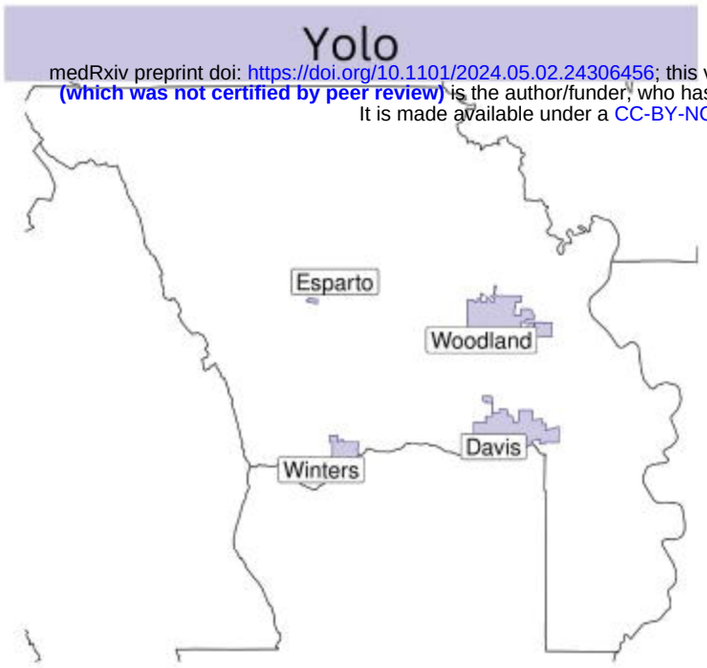

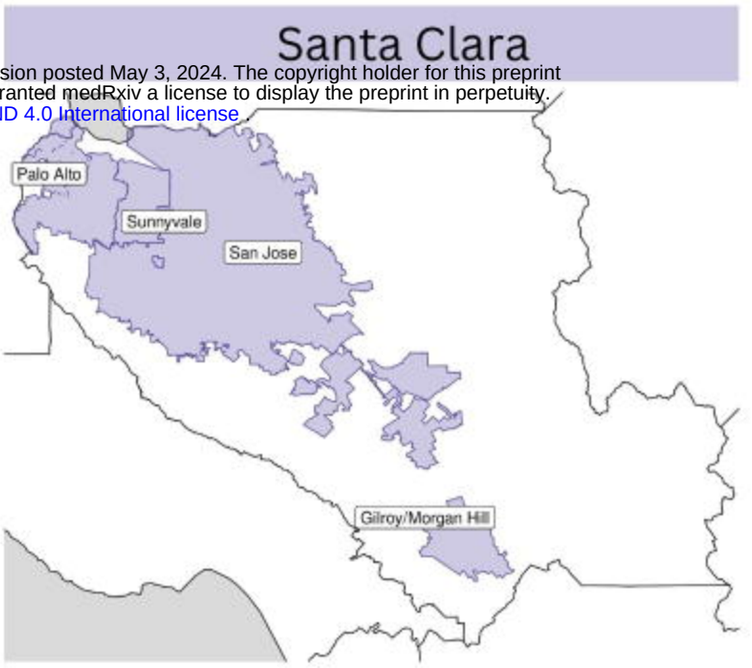

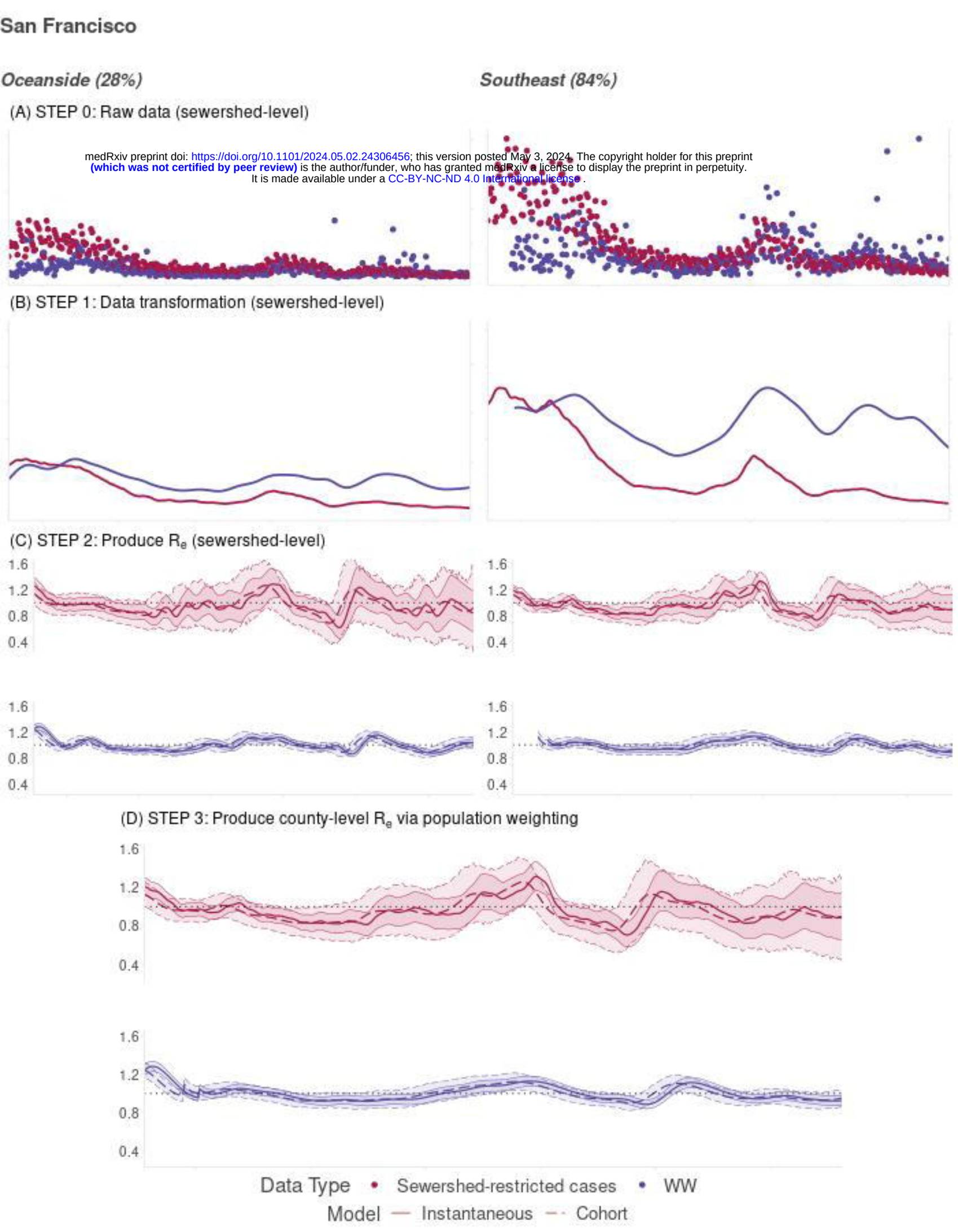

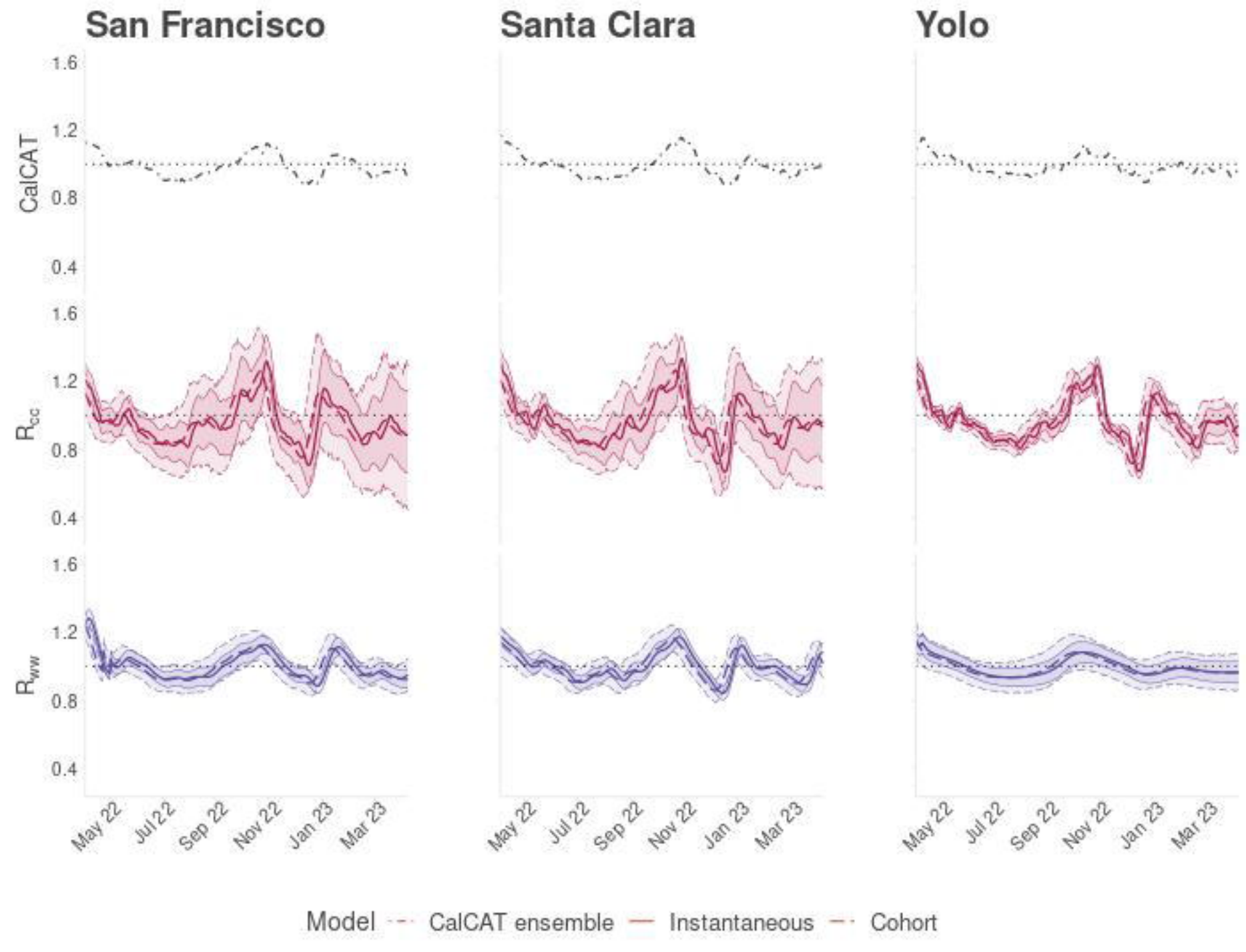
San Francisco
Santa Clara
Yolo
CalCAT
R_{cc}
R_{ww}
1.6
1.2
0.8
0.4
May 22
Jul 22
Sep 22
Nov 22
Jan 23
Mar 23
Model
CalCAT ensemble
Instantaneous
Cohort

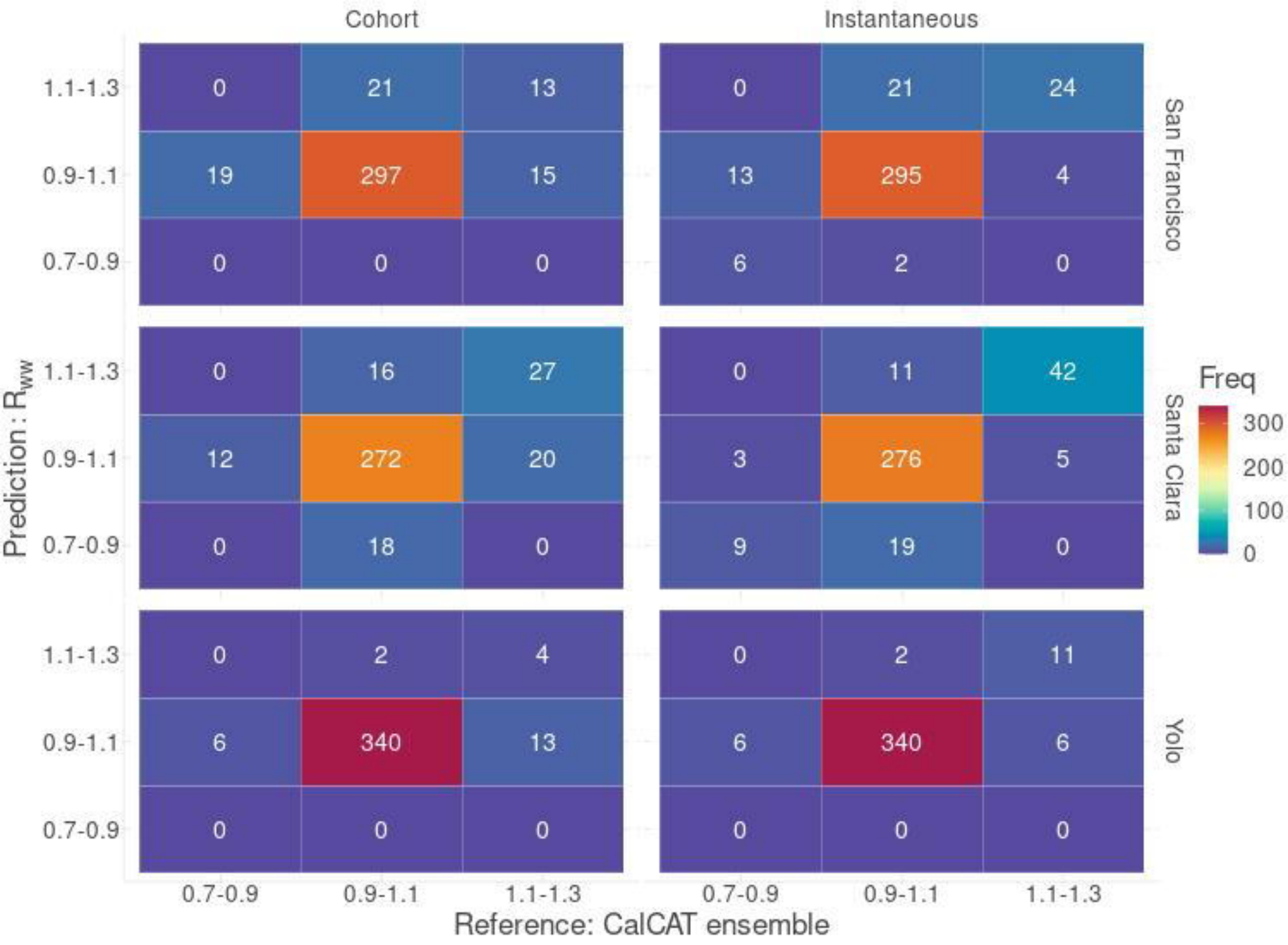
Cohort
Instantaneous
San Francisco
Santa Clara
Yolo
Prediction: R_{ww}
1.1-1.3
0.9-1.1
0.7-0.9
Reference: CalCAT ensemble
Freq
300
200
100
0
0 21 13
19 297 15
0 0 0
0 21 24
13 295 4
6 2 0
0 16 27
12 272 20
0 18 0
0 11 42
3 276 5
9 19 0
0 2 4
6 340 13
0 0 0
0 2 11
6 340 6
0 0 0